ORIGINAL ARTICLE

WAAM-based repair cladding for forging tools: a comprehensive study of wear in laboratory and industrial conditions

Pawel Widomski · Marcin Kaszuba · Maciej Zwierzchowski · Constantinos Goulas · Martijn Bos · Marcel Hermans

Received: 11 February 2025 / Revised: 26 January 2026 / Accepted: 1 February 2026

Abstract

This study explores Wire Arc Additive Manufacturing (WAAM) as a repair method for forging tools, comparing it to conventional H11 tool steel. Laboratory tests were conducted on four samples obtained from different WAAM layers, which are representative of the respective layer positions for hardness and wear tests at room temperature and 500 °C. Chemical composition analysis was performed to verify compliance with tool steel standards, and evaluations included hardness testing at both temperatures, tensile strength assessment, wear resistance measurements (ball-on-disc mode), and hardness mapping to verify layer consistency. The WAAM material exhibited wear factors on the order of 10^{-6} mm³/Nm, below typical literature values reported for H11 tool steel, and showed a clear correlation between layer hardness and wear response. Industrial validation through hot forging trials demonstrated that WAAM-repaired tools achieved 3000 cycles compared to 2500 cycles for conventionally repaired tools, with approximately 60% shorter repair time and 21% lower filler material consumption. These results confirm WAAM as a viable and superior method for cladding and repairing forging tools, offering improved durability, higher efficiency, and reduced use of expensive alloying elements in industrial applications.

Keywords Forging tool · Regeneration · Hardfacing · Wear

1 Introduction

One of the commonly used methods for manufacturing steel products is die forging, particularly applied for key components that affect user safety. To properly carry out the process under industrial conditions, it is essential to use appropriate tools, which, due to the challenging working conditions, such as high surface pressures and elevated temperatures, wear out quickly despite the use of expensive hot-work alloy steels. For this reason, the production costs of forgings are strongly dependent on the durability of the tools. It is generally accepted that the cost of tools consumed during production accounts for 15% to 40% of the total forging production cost [1]. According to other authors, this range is between 5% and 30% [2, 3]. In the case of difficult forgings, where excessive or

https://doi.org/10.1007/s43452-026-01461-1

Published online: 20 February 2026

even destructive wear occurs, the cost can increase to 50% [4]. Global die-forging production in 2023 amounted to approximately 20 million tons [5], indicating significant demand for durable and efficient forging tools.

Forging tools undergo wear due to the impact of various destructive mechanisms, whose contributions vary depending on the specific process. As the forging industry has developed and sought suitable manufacturing methods for tools, a substantial amount of research has been conducted analyzing the mechanisms that cause their wear. The effects of individual wear mechanisms, such as abrasive wear [6, 7], fatigue cracking [8], or plastic deformation due to tempering of the die surface under high temperatures [9], have been described. The influence of cyclic thermal loads, leading to thermal-mechanical fatigue in the tools, has also been studied [10]. Research has also been conducted on wear during the first five forging cycles, which is fundamental to the overall durability [11]. More detailed studies focused on the combined influence of all mechanisms and were presented in works [12] and [13].

The primary wear mechanisms on forging dies—including abrasion, thermal-mechanical microcracking, and surface tempering—are limited to the near-surface layer (a few millimeters), making them suitable for regeneration through mechanical removal and reapplication of material; however, internal fatigue cracking remains difficult to control and leads to complete die destruction. The high cost of tool steel for manufacturing dies via machining encourages regeneration methods, which are particularly economical for medium and large forgings where production series are small and dies represent significant investment costs. Advanced machining techniques and modern welding technologies now enable cost-effective die regeneration by precisely removing worn surfaces and replacing them with newly applied layers.

Currently, there is a strong emphasis in the industry on reducing the negative environmental impact by striving to limit the consumption of raw materials, which could lead to increased procurement costs and negatively affect future price growth [14]. By achieving goals in an appropriate way and ensuring sustainable development, industrial products will be affordable and environmentally friendly [15]. In recent years, the idea of reusing materials from existing products, referred to as the circular economy, has emerged [16]. The practical implementation of such a strategy requires a change in thinking about the product life cycle by planning material recovery already at the design stage [17]. In this case, forging tools can be considered an internal-use product, over which the manufacturing plant has control and discretion throughout the entire cycle, from design to disposal.

Since repeated machining is limited by minimum die height, regeneration—which restores the die to its original height through disassembly, cleaning, inspection, rebuilding, reassembly, and testing—provides a more viable solution for extending die life [18]. Rebuilding is the most critical part of regeneration, as it determines whether the regenerated tools will return to their original properties or even improve them [19, 20].

Die regeneration methods commonly restore the original shape before final machining, with overlay welding being a widely used, high-productivity technique employing coated electrodes primarily in manual or semi-automatic processes [21]. This approach efficiently repairs forging dies by applying large amounts of filler material, although its applicability is limited by the need for skilled operators and simple manipulators [22].

Newer welding methods show greater potential for automation, leading to higher process stability and resulting in products of better quality. One such method is welding with a non-consumable tungsten electrode, which is characterized by a stable arc and does not cause splattering. Its lower productivity compared to other methods is offset by the high quality of the resulting welds, which are homogeneous and free from porosity. This method is successfully used to weld metal alloys significantly different in chemical composition and properties from the steel substrate, such as cobalt (stellites) and nickel, which have much higher temperature resistance [22–24]. Intensive research is also being conducted to increase surface resistance through selective overlay welding, dividing zones into areas where combinations of materials with high hardness are used, with a transition zone to reduce the effects of thermal fatigue due to different thermal expansion, and materials with high ductility and crack resistance [25, 26]. The modification of working surfaces in this way is described in other works as building gradient and bimetallic layers [27, 28].

A separate category of welding technologies uses ion beams or laser power to melt metal, enabling easy automation through complex digital control systems that integrate with modern machines for high efficiency, reduced unnecessary operations, and improved quality and repeatability. Beam technologies naturally lend themselves to additive manufacturing, allowing successful regeneration of tools or even creation of new ones from scratch [29–31]. This allows the production of complex shapes that would be difficult to achieve otherwise [32, 33]. An interesting example of using laser cladding additive technology is the production of dies with internal curved cooling channels in the most thermally stressed areas, shapes that are impossible to obtain using standard straight-line drilling [34–36].

To successfully implement tested solutions in industry, promising laboratory results are not enough; they must also be given a form that allows them to compete effectively with other currently used methods. Just as computer-aided manufacturing has completely dominated machining, all regeneration methods using overlay welding must be automated, limiting human influence on the final result. The first step is to use robots to manipulate the welding device and traditionally program them before starting work, without real-time control [37]. The next step will be the use of collaborative robots, and the final solution should be fully automatic welding with minimal human involvement [38]. Ongoing research and industry trends indicate that the further development of regeneration processes will involve increasingly replacing manual labor with automated workstations using additive technologies [39].

The limitations of current forging die manufacturing highlight the potential of Wire Arc Additive Manufacturing (WAAM), which allows printing only the necessary material and eliminates rough CNC machining. WAAM not only enables die production but also multiple repairs by reprinting worn surfaces, significantly extending die lifespan; given that forging dies can constitute 15–30% of the total hot-forged product cost, extending their life with WAAM could greatly impact the forging industry [13, 40].

Wearfacing and die repair commonly use gas tungsten arc welding (GMAW), which requires certified, highly skilled welders and preheating due to the complex, locally varying damage that demands different repair measures. The unique geometries of forging dies make automation advantageous, as laser scanning systems can detect defects by comparing the current die surface with original CAD data, and combined with process monitoring, automated toolpath generation, and machine learning, ensure consistent, high-quality welds—critical for uninterrupted operation of large dies [41].

As there is no universal wear test, a method should be developed that accurately predicts final wear properties with minimal effort. Forging dies require a balance between high hardness for surface wear resistance and high toughness for core impact resistance, suggesting an optimal combination of a hard surface with a tough core [1, 42].

According to observations by Kim et al., very few articles on WAAM of tool steels were published before 2018. However, in recent years, significant interest in this technology has emerged, as demonstrated by several key contributions to the field between 2018 and 2024 [43]. Kim et al. investigated the effect of shielding gases on WAAM of 5Cr-4Mo tool steel for die casting molds, establishing foundational parameters for the process [43]. Hackenhaar et al. explored different current deposition modes in WAAM of AISI H13 tool steel, demonstrating the influence of welding parameters on mechanical properties [44]. Research by Tanvir et al. examined phase stability and mechanical properties of WAAM-deposited H13 tool steel at elevated temperatures, addressing critical performance requirements for industrial applications [45]. Wang et al. investigated the microstructure and properties of die steel fabricated by WAAM using H13 wire, confirming the viability of WAAM for die applications [46]. Finally, Baffa et al. studied the effects of stepover and torch tilting angle on WAAM repair processes, advancing the understanding of process optimization for tool regeneration [47]. These works collectively demonstrate growing research interest in WAAM for tool steel applications, driven by the technology's potential for both manufacturing and repair of forging dies.

This study addresses the current gaps in the literature by adopting a holistic and systematic approach that combines three key elements: (1) comprehensive laboratory characterization of WAAM-produced tool steel under controlled conditions, including hardness and wear resistance testing at both room temperature and elevated temperature (500 °C) simulating hot forging conditions; (2) microstructural investigations of the WAAM material from different layers to confirm technological capability and consistency for tool repair applications; and

Table 1 Chemical composition (wt%) of used applied materials

Material type	C	Si	Mn	Cr	Mo	V	W	Fe
Fe-Fe4MC2	0.25–0.30	0.40–1.00.40.00	0.50–0.90	5.0–6.0	2.0–3.0	0.5–0.9	1.8–2.7	balance
Robotool 46 (wire used for conventional repair)	0.2	0.50	0.90	5.10	3.8	0.25	-	balance
H11 steel (base material)	0.32–0.42	0.8–1.2	0.2–0.5	4.5–5.5	1.2–1.5	0.3–0.5	-	balance

Table 2 Parameters of GMAW hand welding processes

Welding process	138 (welding with powder wire with a metal core)
Dimension of the binder [mm]	1.6
Current [A]	Bead number: 1–175.2–275
Arc voltage [V]	Bead number: 1–21.2–29.5
Type of polarity	DC+
Hardfacing speed [cm/min]	30
Shielding gas	ISO 14,175 – M14 – $ArCO_2$ – 5/2
Gas flow speed [l/min]	13–20
The length of the free wire outlet [mm]	11–20
Angle of welding torch adjustment	Perpendicular to the hardfaced surface
Preheat temperature [°C]	350
Interpass temperature [°C]	400
Number of padding weld layers	2
Thickness of the obtained padding weld	4–6 mm

(3) industrial validation through real hot forging trials, directly comparing the performance of WAAM-repaired tools with conventional H11 steel tools. This integrated approach, encompassing both fundamental material studies and practical industrial testing, represents an innovative contribution to the existing body of knowledge on WAAM of tool steels, moving beyond purely laboratory-based studies to demonstrate the viability and superiority of WAAM for industrial tool regeneration.

The knowledge mainly concerns the materials geometrical response and its wear-resistance at elevated temperatures. Understanding the geometrical response will help to generate printing paths that are highly optimized for the forging die's unique geometry and staying close to forging dies tolerances. Next to tolerances should the optimized toolpaths also consider the local wearfacing operations. Knowing the materials wear properties for different weld heat inputs and heat treatments will help to predict and print the desired microstructure.

2 Materials and methods

2.1 Material selection

The study involved two materials, namely hot work tool steel obtained by Wire Arc Additive Manufacturing (WAAM) and conventional hot work H11 steel. For the WAAM process, welding wire AM Fe-Fe4MC2 supplied by Lincoln with a chemical composition presented in the Table 1 was used:

2.2 Conventional cladding (GMAW) process parameters

Cladding was performed on a manual welding station equipped with an automatically controlled positioner on a single axis. The tools were preheated, and the interpass temperature was maintained. The process was carried out according to best practices and welding qualifications, using Robotool 46 wire produced by Welding Alloys on an H11 steel substrate. The key welding process parameters are listed below in the Table 2.

2.3 WAAM process parameters

A TechMan (TM) cobot integrated with a Miller welding system driven by the MaxQ repair software at RAMLAB was used. Table 3 gives an overview of the hardware that was used.

The digital repair workflow, which includes automatic scanning, toolpath generation, and quality-monitored deposition is described. The MaxQ repair system, developed in-house by RAMLAB, was utilized for this purpose. The automatic repair solution follows these steps, after the necessary preparations such as acquiring geometric information, performing mechanical and chemical cleanings, and preheating the materials. The key welding process parameters have been classified as they constitute the company's know-how. Below, the subsequent stages of the preparation and automatic path generation process in the WAAM process are outlined.

1. A 3D model of the target volume is loaded into MaxQ repair software.
2. A scan of the damaged die is made and aligned with the target volume.
3. The toolpaths to repair the die are automatically calculated together with the boundary conditions such as the repair volume, process parameters and cobot physical constraints.
4. The die is repaired using the automatically generated toolpaths based on the scanned data.

a. Each layer is projected onto the previous layer using the MaxQ 3D camera.
b. Before printing each layer the temperature of the part is monitored using the MaxQ temperature sensor to maintain a proper interlayer temperature.

To reduce the risk of cracking, a preheating step is implemented before the material deposition begins. Heating elements are strategically positioned on the sides and bottom of the die. The preheating temperature is set at 300 °C, with a maximum heating rate of 100 °C per hour. To prevent heat loss to the ambient, rock wool is used to insulate the die for keeping the heat effectively.

After completing the repair process, the heating box is closed, enclosing the die inside. Subsequently, Post Weld Heat Treatment (PWHT) was carried out following the data sheet provided by Lincoln Electric for the wire used. After PWHT, the die was allowed to cool inside the heating box until it reached room temperature. Finally, the die was taken out of the box after 24 h to undergo final inspections.

2.4 Sample preparation

For the WAAM process, prior to cladding the demonstrative tools, a sample in the form of an additively clad (printed) block with dimensions of $300 \times 600 \times 100$ mm was prepared. The sample was used to investigate the structure and material properties to confirm its suitability for industrial applications. After printing, the sample

Table 3 Hardware and software used in WAAM process

Hardware specifications	Value
Robot	Panasonic TM12
Reach	1300 mm
Payload	12 kg
Weld source	Miller Auto-Continuum™ 350
Welding torch	Tregaskiss® Air-Cooled MIG Guns, TOUGH GUN® CA3 Series, robotic air-cooled MIG Gun
Pre-heating source	GlobeHeat 10.5 kW inverter power source (GHT1232)
Heating elements	3x Flexible Insulated Preheater 60 V (GHT5502)
MaxQ repair key unit	
MaxQ control box	Integrated PC, electric cables, database server
MaxQ 3D scanner	Zivid 2
MaxQ temperature sensor	Optris Xi80 thermal camera

 https://doi.org/10.1007/s43452-026-01461-1

was cut into smaller sections, and then samples for individual tests on microstructure and material properties were extracted from it.

Rectangular samples were cut from the block of each material. Each sample was cut in such a way that two pieces were obtained from each layer. One sample was positioned transversely to the direction of the weld bead, while the other was aligned with the direction of the weld bead. Figure 1 below shows a view of a sample printed using the WAAM method, with the direction and location of each sample cut marked.

Samples extracted from the deposited block were not subjected to any post-cutting heat treatment or surface treatment to ensure that the material properties reflected the as-deposited state. Sample preparation for microstructural and mechanical testing involved standard grinding and polishing procedures. For microstructural examinations, prepared samples were etched with 3% Nital solution to reveal the material's internal structure and phase distribution.

2.5 Tests performed on the samples

Chemical composition analysis was performed using X-ray fluorescence (XRF) spectrometry on samples extracted from each material (WAAM-deposited material and conventional H11 steel). The XRF analysis was conducted in accordance with ISO 14,975 standard using an Olympus Vanta measuring device, to ensure quantitative determination of elemental composition. Each sample was analyzed in triplicate to ensure repeatability of measurements, and results were averaged for final composition determination.

Hardness measurements at room temperature and 500 °C were performed using a PRUFTECHNIK inverted Rockwell hardness tester, equipped with a furnace with a maximum operating temperature of 600 °C. A standard HRC indenter from Dialex, designed for measurements at elevated temperatures, was used.

Vickers hardness measurements were performed with a 100 g load applied for a dwell time of 10 s. Hardness mapping was conducted across the cross-section with 0.5 mm spacing between indentations, resulting in a minimum of 10 measurements per sample. Hardness measurements was carried out using the LECO AMH45 Automated Hardness Testing Machine, equipped with hardness mapping software, a camera, and an automated stage with autofocus.

Optical microscopy studies were performed on an Olympus GX51 microscope equipped with a set of objectives ranging from 5x to 100x and an optical system with a 10x camera. The examinations were conducted in bright field. The samples were prepared for testing by standard grinding and polishing, followed by etching with 3% Nital.

Wear tests were carried out in ball-on-disc mode using an Rtec Multi-Function Tribometer MFT-5000 equipped with an integrated profilometer. An Al_2O_3 ball with a diameter of 6 mm was employed as the indenter. The tests were conducted under room temperature conditions with a 10 N load, 0.1 m/s linear velocity, 3 mm radius, and a sliding distance of 250 m. Sliding wear tests were conducted on four samples extracted from different layers of

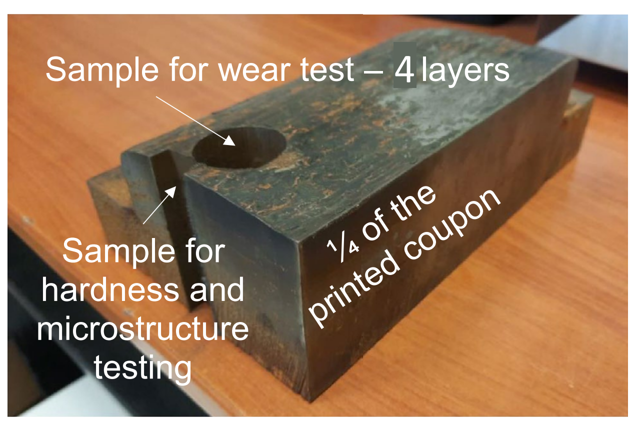

Fig. 1 View of a sample printed using the WAAM method

the WAAM deposited coupon. Each sample was tested once under identical conditions, yielding four independent measurements representing wear behavior at different heights within the deposited material. Each sample was measured using the integrated optical profilometer after every one-quarter of the sliding distance (62.5 m) and once more at the end over at least eight cross-sections to ensure statistically representative data. The results comprised plots of the coefficient of friction versus sliding distance, the wear factor K, and optical profilometer profile maps for each sample.

Wear tests under dry friction conditions and room temperature were conducted to: (1) obtain repeatable, controlled laboratory conditions, and (2) enable comparison of results with literature, where many studies of AISI H11 are conducted under identical room temperature conditions. However, we are aware that proper operating conditions (high temperature, significant normal loads) would significantly affect the wear characteristics of both materials. Therefore, the laboratory test results must be interpreted as relative data indicating the ability of WAAM material to compete with reference H11 material under standardized experimental conditions, rather than as a full prognosis of material behavior under real forging conditions.

All tests were conducted under ambient conditions. The test conditions were chosen to replicate the loading conditions that prevail in forging processes in terms of pressure and friction. To ensure a reliable comparison between conventional and WAAM steel, additional hardness measurements were performed at elevated temperature. Moreover, industrial-scale tests, described in Sect. 2.7, were also carried out, further strengthening the credibility and robustness of the obtained results.

2.6 Analysis of the regeneration process of forging tools using the conventional method and the WAAM technology

To evaluate the added value brought by the use of the robotic WAAM cladding technology, comparative analyses were conducted by scanning the surface of the tools prepared for cladding and the surface of the tools after cladding.

Next, a comparison of the surfaces was conducted, and the volume of material deposited in both processes was determined. The volume was converted into the weight/mass of this material, and based on this, the amount of material used in the process was estimated (naturally, the actual consumption of welding wire is proportionally higher and depends on various factors).

A comparison was also made in the context of the size of the allowances left for mechanical machining. This comparison is important as it evaluates the ability to replicate the target shape in the cladding process and confirms the possibility of eliminating unnecessary allowances.

2.7 Performance tests of repaired tools in industrial forging conditions

The next stage involved tests conducted under industrial conditions. These were tests in the hot forging process, where tools previously repaired were tested for a specified period and were then withdrawn to compare their wear.

For the study, a hot forging process of steel forgings made from steel S355J2 with a mass of 6,57 kg (Fig. 2a) was selected. The forgings are produced using a Massey 2500 T press with a maximum force of 25 MN, utilizing dies. From all the tools (dies) involved in the process, the lower preliminary die, with dimensions of 600 × 245 × 155 mm and a mass of 211 kg, was selected for testing, and its model is shown in Fig. 2c. The tools in this process are subjected to high pressures, intense friction between the forging and the tool surfaces, and operate at elevated temperatures. Although thermographic analysis indicates that the temperature is at least 230 °C at the moment the forging is removed from the die surface, it should be assumed that the temperature is at least 400 °C (Fig. 2b).

The tests included scanning before forging, hot forging, and scanning after the forging process. By comparing the scans, the size of the material losses was detected, and the observed wear was further discussed.

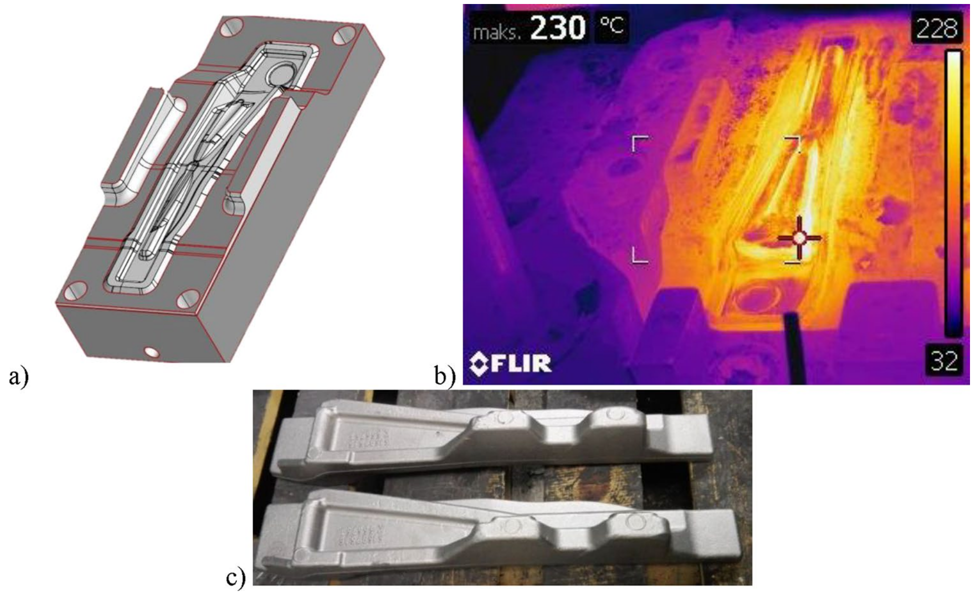

Fig. 2 **a** Tested tool - lower die (CAD model), **b** thermogram view of the tool immediately after removing the forging from the surface, **c** forging from the analyzed forging process

The industrial test results are derived from single measurements for each repair technology and should be interpreted as preliminary data indicating the potential of WAAM technology.

3 Results

3.1 Results of the laboratory tests performed on the samples

The tests on the samples were conducted with consideration of the successively applied layers to obtain averaged properties and detect any discrepancies resulting from the incremental deposition of layers. For each of the four cladding layers, an analysis of the influence of temperature on hardness (HRC) was performed. HRC hardness tests were conducted at room temperature and at 500 °C. The hardness tests were carried out using an inverted Rockwell hardness tester, equipped with a furnace capable of conducting tests up to 600 °C.

The obtained results are presented in Fig. 3. It can be observed that despite slight differences in hardness at room temperature, each layer shows lower hardness at 500 °C. The highest hardness at 500 °C was recorded for layer no. 1, measuring 41.9 HRc, while the lowest was recorded for layer no. 2, measuring 32.8 HRC.

The hardness at room temperature ranges between approximately 43–51 HRC, and at elevated temperatures between 30 and 42 HRC, which is an excellent result for materials operating at high temperatures.

A hardness mapping analysis using the Vickers method was performed across the entire cross-sectional surface with a 100 g indenter load and a 0.5 mm spacing between the indentations. The results are presented in Fig. 4. It can be observed that the highest hardness is found in the final layer, which is the surface of the cladded material. Each subsequent layer shows lower hardness in the range of 300–600 HV. Another significant observation is the uneven hardness resulting from the nature of the cladding layer manufacturing process—tempering and layer-by-layer strengthening of the material. The very high hardness in the surface layer, above 700 HV, is an excellent result, indicating the suitability of the selected method and material for cladding elements operating under friction at elevated temperatures.

The lower hardness observed in layers 2 and 3 (approximately 32–33 HRC at 500 °C) is attributed to secondary tempering resulting from repeated thermal cycling during the WAAM deposition process. Specifically, layers 2 and 3 were subjected to high temperatures during the deposition of subsequent layers. During these heating cycles, the cooling rate was not sufficiently intensive to permit re-hardening; instead, the material underwent

Fig. 3 The hardness of individual layers at room temperature and at 500 °C

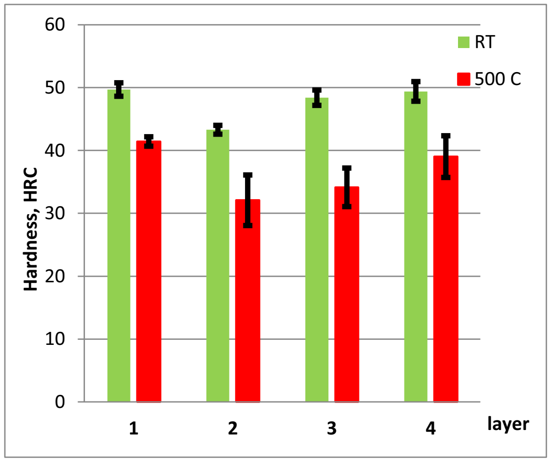

No. of layer	HRC in RT	HRC in 500°C
1	49.0 51.1 49.7	40.6 41.8 41.9
2	42.5 43.9 43.3	27.7 35.7 32.8
3	46.8 49.2 48.4	35.1 36.6 30.7
4	46.8 46.6 49.4	35.2 41.2 40.7

3

Fig. 4 The distribution of microhardness across the cross-section performed for all cladded layers

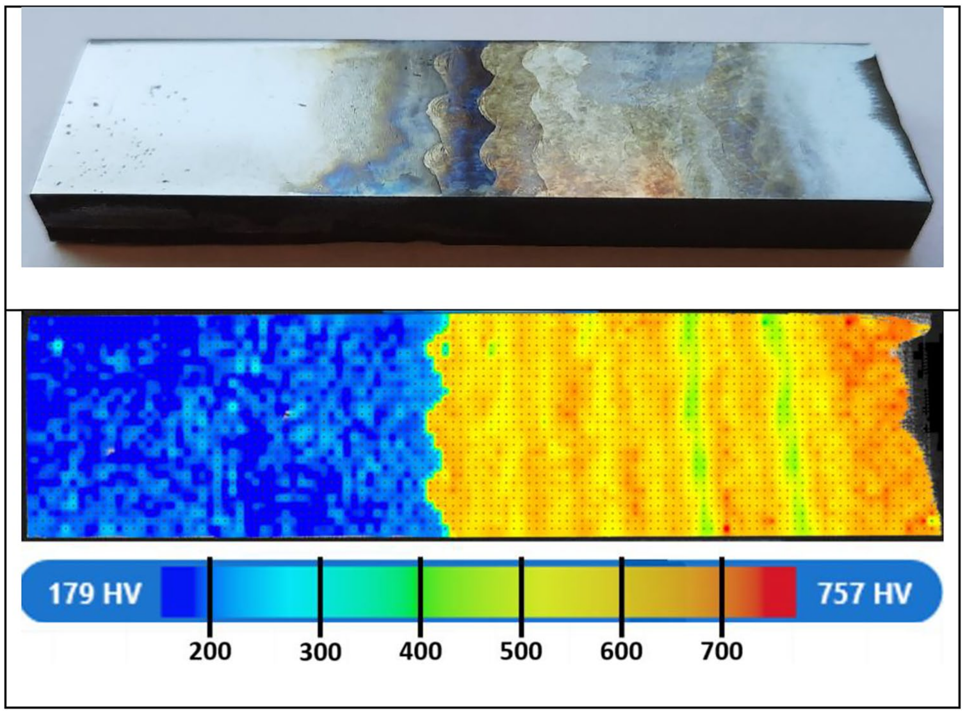

tempering, leading to reduced hardness. The localized hardness reductions observed in the hardness mapping are evidence of this tempering phenomenon, which is inherent to multi-layer additive manufacturing processes where excessive heat input and relatively slow cooling rates in the intermediate layers result in microstructural changes that reduce hardness. This effect demonstrates a key limitation of the WAAM process: the accumulation of thermal energy in intermediate layers during the deposition of subsequent passes.

A control spectrometric analysis of the coating was performed. The results confirm that the composition of the cladding falls within the specification. The base material is iron—approximately 87.7%, along with alloying elements such as Cr, Mo, W, Mn, V, Ti, and trace amounts of Ni and Cu Table 4.

Microstructural analysis was conducted for the discussed multilayer reference sample (Fig. 5. The microstructure of the substrate is ferritic-pearlitic steel. The cladding layers consist of carbide precipitates in an alpha-iron matrix for the transition layers, while the surface layer has a fine-grained microstructure with relatively high hardness. The microstructure is composed of very fine carbide precipitates with high dispersion. Due to the effect of

Springer

Table 4 The result of the chemical composition analysis of the material from the sample deposited by WAAM technology

Hardfacing material Fe based – wt% (Lincoln wire) additional: 0.07 wt% Ni and 0.06 wt% Cu									
C	Mn	Si	P	S	Cr	Mo	V	W	Ti
0.32	0.72	1.03	< 0.03	< 0.03	5.79	2.42	0.60	2.41	0.17

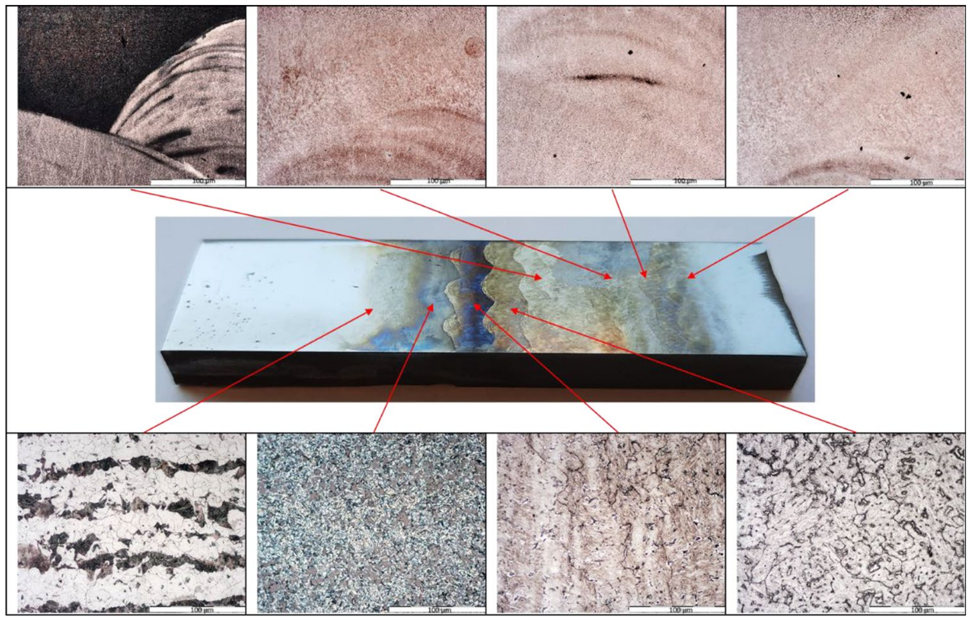

Fig. 5 Microstructural analysis of the sample produced using WAAM technology

temperature, these precipitates coagulate, which is visible in the lower layers. The microstructure is typical and characteristic of materials resistant to wear, operating at elevated temperatures.

Sliding wear tests were conducted on four samples extracted from layers at different heights throughout the deposited structure. The tests revealed a consistent friction coefficient of approximately 0.85 across all samples, as presented in Fig. 6. This uniformity in friction behavior indicates stable tribological properties regardless of sampling location within the WAAM deposit. The friction coefficient exhibits rapid initial rise during the first ~ 2,000–6,000 s, followed by stabilization to a plateau value around 0.85–0.90, which is characteristic of adhesive wear mechanisms in tool steel contacts.

In Fig. 6, stops are visible at every ¼ of the friction path (every 62.5 m), which was intentional, as a wear-profile inspection was performed during each of these pauses.

The wear profiles displayed in Fig. 7 (a-d) reveal distinctive surface topographies following the ball-on-disc sliding tests.

All profiles exhibit symmetric cross-sectional geometries, characteristic of classical abrasive wear mechanisms. Notably, the wear profiles display pronounced grooves perpendicular to the sliding direction at the profile depths, which is consistent with the typical morphology of three-body abrasive wear. The profiles obtained from samples at different heights show varying wear depths, reflecting differences in the microstructural integrity of successive layers within the WAAM deposit. Layers 2 and 3, according to their lower hardness relative to layers 1 and 4, exhibit distinctly deeper wear grooves and greater material removal volumes, demonstrating the strong correlation between hardness and wear resistance in this material system. Based on the values measured with the profilometer, the friction coefficient K was calculated and is presented graphically in Fig. 8 below.

Based on the measured wear track geometries, the wear factor K was determined for each layer. The values, expressed in exponential form, are as follows:

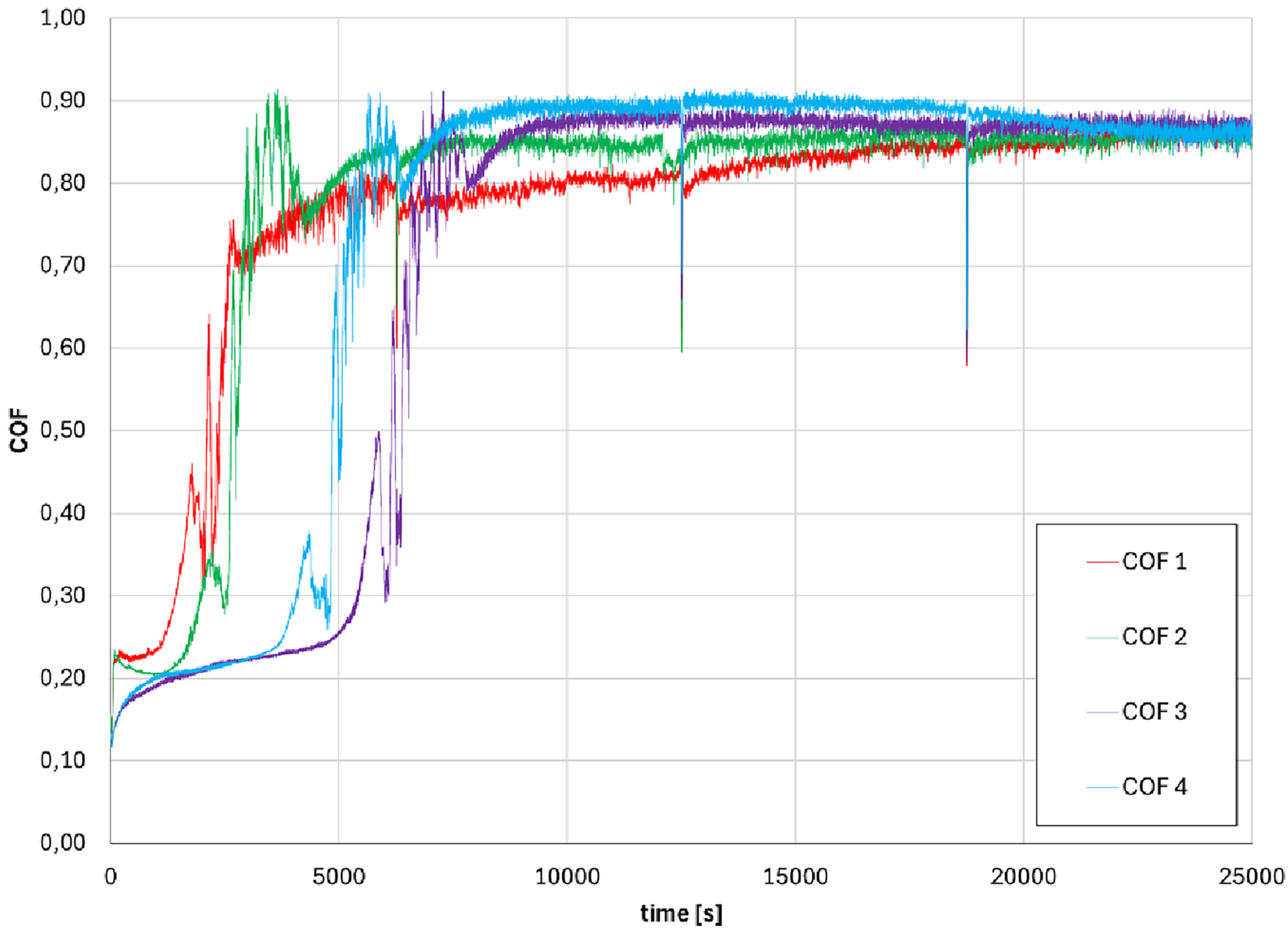

Fig. 6 Coefficient of friction values as a function of sliding distance for each of the four layers

- layer 1–2.39 × 10^{-6} mm³/Nm,
- layer 2–8.48 × 10^{-6} mm³/Nm,
- layer 3–8.92 × 10^{-6} mm³/Nm,
- layer 4–6.90 × 10^{-6} mm³/Nm.

All results are of the same order of magnitude, but clear differences between layers are visible. Layers 2 and 3, which exhibit lower hardness, also show the highest wear factors (above 8 × 10^{-6} mm³/Nm), whereas layer 1 has the lowest value, with layer 4 at an intermediate level. These differences are statistically significant while remaining consistent within the experimental scatter. In comparison, Drozd et al. reported a wear factor of approximately 3.67 × 10−53.67 × 10–5 mm³/Nm for uncoated H11 (X37CrMoV5-1) steel under ball-on-disc testing at room temperature and a 10 N load the WAAM-deposited material exhibits a wear factor lower by about one order of magnitude than reference H11, indicating clearly superior sliding wear resistance. Such behaviour can be attributed to the modified chemical composition of the WAAM wire, enriched in alloying elements that promote the formation of hard phases and thus improve wear performance.

.

 https://doi.org/10.1007/s43452-026-01461-1

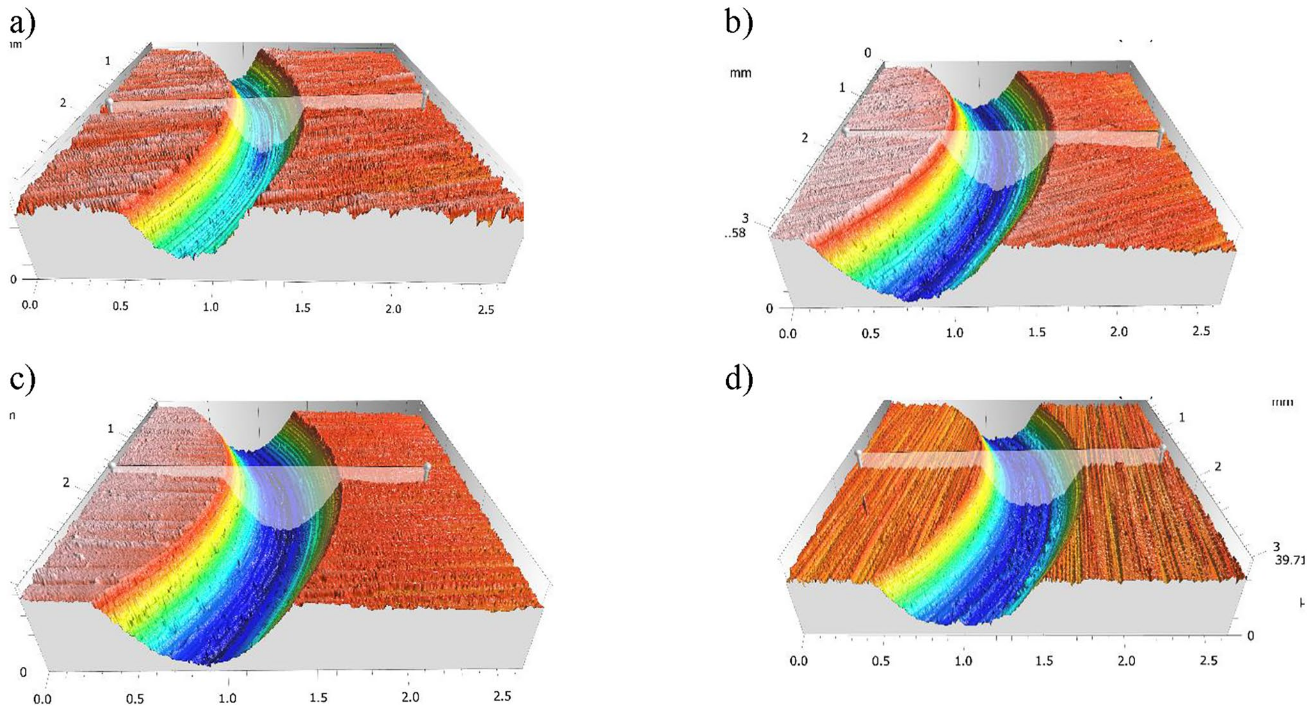

Fig. 7 Plot of the friction coefficient values together with the measured data and standard deviation for each of the four layers

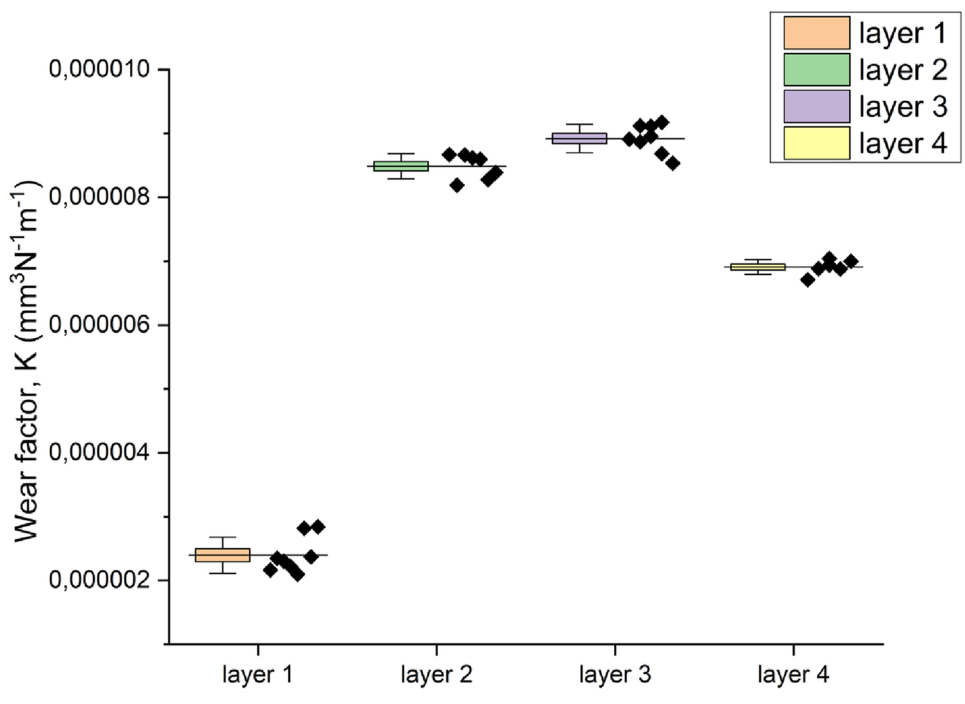

Fig. 8 Plot of the friction-coefficient values together with the measured values and standard deviation for each of the four layers

3.2 Comparison of repair welding of tools by conventional GMAW and WAAM processes

In accordance with the previously described technology, regenerative cladding trials of forging tools were conducted using two methods. In both cases, the tools were pre-milled to remove the worn-out layer. Then, in the cladding process, the missing material was restored, including an allowance for machining. In the manual

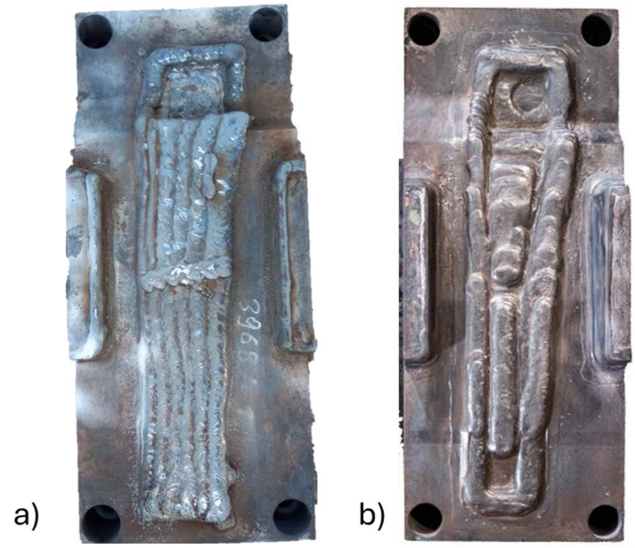

Fig. 9 View of tools after regenerative cladding, (**a**) manual cladding using the GMAW method, (**b**) robotic cladding using the WAAM method

Table 5 Results of volume and mass calculations for the cladding and allowance

Padding weld volume	Conventional repair (GMAW)	Grade2XL concept (WAAM)
	882 198 mm^3	700 617 mm^3
Padding weld weight	6,97 kg	5,53 kg
Machining allowance (volume)	545 354 mm^3	365 662 mm^3
Machining allowance (weight)	4,31 kg	2,89 kg
Lead time for 1 repair	28 h	11 h

GMAW cladding method, a weld with regular shapes was produced, while in the WAAM technology, it was possible to create a weld with shapes more closely resembling the target die geometry. The illustrations of both dies are shown in Fig. 8.

To more accurately assess and compare both methods, scanning and volume measurement of the cladding and the remaining allowance for subsequent mechanical machining were conducted. For easier interpretation, the results of this measurement are presented in Fig. 9. These results are also summarized in Table 5.

The analysis of the volume and mass of the cladding, as well as other changes introduced into the regeneration process by the use of robotic WAAM technology, led to the following valuable conclusions::

- 60% faster repair (from 28 h to 11 h).
- Superior wear and temperature resistance due to WAAM graded repair.
- Faster repair and repeatability of the remanufacturing process (due to automation).
- 21% less material use; 7 times less CRM (Nb) use.
- 59% cost reduction per forging die repaired.

3.3 Performance test in industrial forging process

The tool trials in the forging process demonstrated the correct functioning of the forging die repaired using WAAM technology. Additionally, 20% more forgings were produced with relatively much lower wear values. This wear was measured by comparing the tool scans before and after operation. The results of these measurements are shown in Fig. 10,11.

The wear measurement results confirmed another benefit of using robotic cladding technology—an improvement in die durability during the forging process. It is evident that the wear is more uniform, and for the WAAM

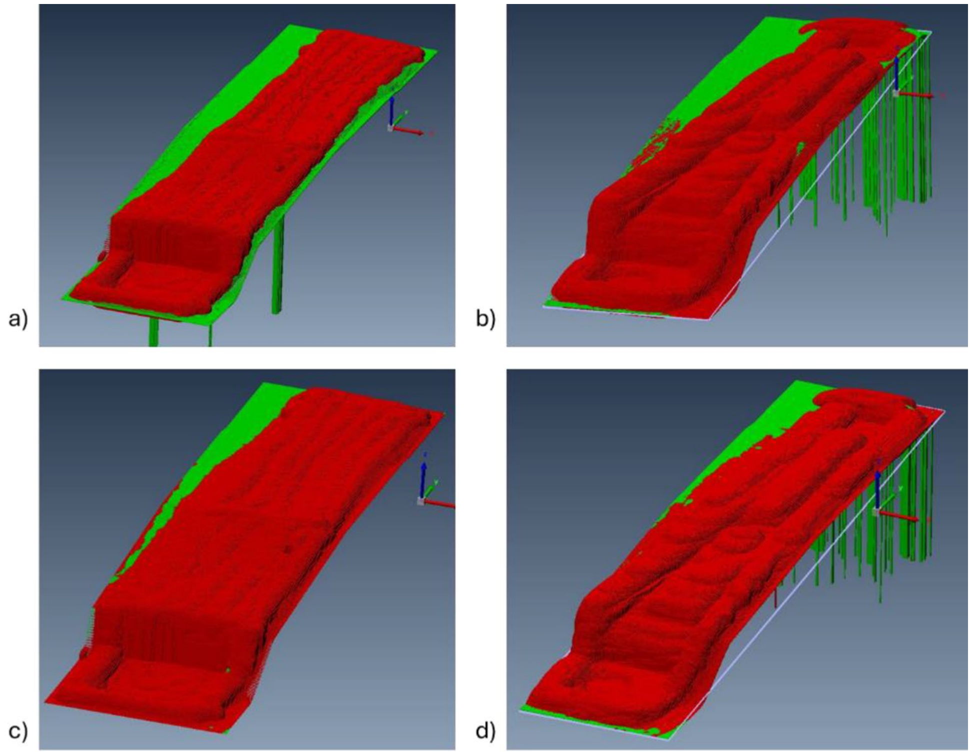

Fig. 10 Volume analysis results, (**a**) cladding by manual GMAW method, (**b**) cladding by robotic WAAM method, (**c**) allowance by manual GMAW method, (**d**) allowance by robotic WAAM method

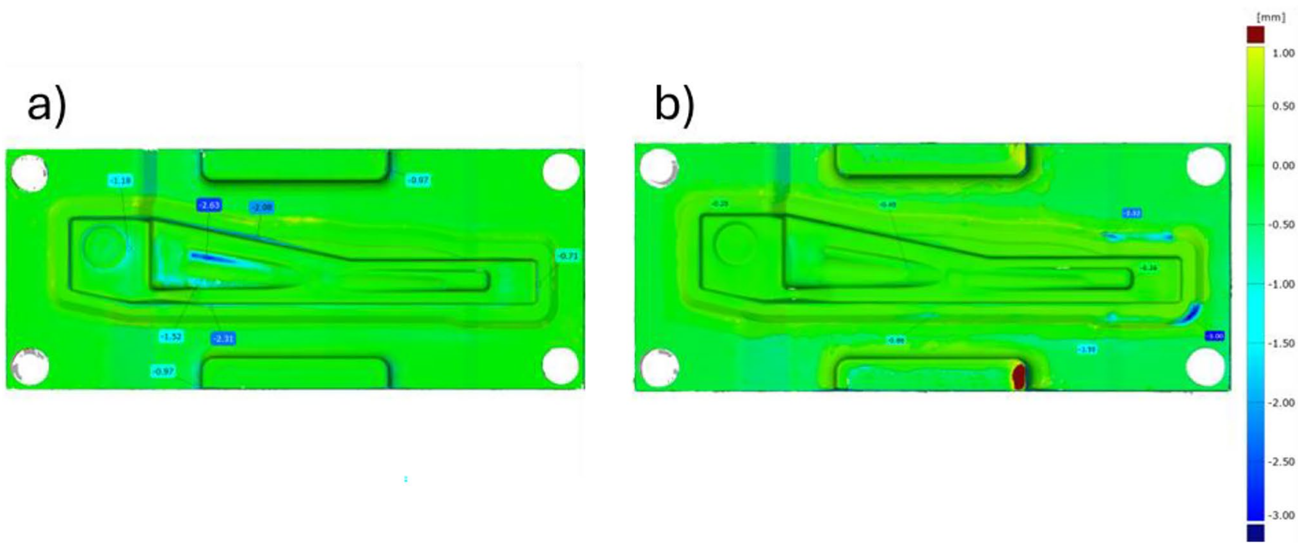

Fig. 11 **a** Conventional repair - forging die after about 2500 pcs., **b** WAAM repair - forging die after 3000 pcs

die, it is lower, not exceeding 0.5 mm (in some areas outside the working cavity, the thickness is greater, which is not due to wear but rather incomplete restoration of those areas during cladding)Fig. 11.

4 Summary and conclusion

This study provides a comprehensive, multi-scale evaluation of Wire Arc Additive Manufacturing (WAAM) as a repair and cladding solution for hot forging tools, integrating laboratory testing, microstructural analysis, and industrial validation to benchmark the technology's performance against both the state-of-the-art and conventional H11 tool steel. Through a series of tribological, mechanical, and microstructural assessments carried out at both ambient and elevated temperatures, the research demonstrates that WAAM-fabricated tool steel consistently exhibits mechanical properties and wear resistance that meet or surpass those of conventional reference alloys, validating its utility for the most demanding industrial applications.

The multi-layer laboratory wear tests demonstrate clear evidence of the tribological performance of the WAAM material. Measurements of the wear factor across the four deposited layers showed values within the range of 2.39–8.92 × 10^{-6} mm³/Nm, with the maximum wear factor remaining substantially lower - by approximately one order of magnitude - than typical literature values for wrought H11 tool steel, such as 3.67 × 10^{-5} mm³/Nm reported by Drozd et al. [48]. Layer-dependent variations in wear resistance were directly correlated with measured hardness profiles, confirming the expected relationship between microstructural integrity and tribological performance. This superior tribological performance can be attributed to the WAAM wire's tailored alloy composition, which is enriched in carbide-forming elements and designed to enhance both hardness and wear resistance at the microstructural level.

Microstructural observations confirmed the presence of finely dispersed carbides within a martensitic matrix, particularly in the uppermost layers, contributing to exceptional high-temperature performance. Transitions in hardness and microstructure with increased build height - resulting from the cumulative effect of thermal cycles during multi-layer deposition - were clearly linked with observed variations in wear behavior.

Industrial-scale tool trials validated the laboratory findings: WAAM-repaired forging dies consistently outperformed dies repaired with conventional GMAW, achieving **20% longer service life** (3,000 cycles versus 2,500 for the reference tool) in representative hot working conditions (hot die forging proces at tool temperatures 300–400 °C). In addition to enhanced durability, automated WAAM delivery resulted in **60% reduction in repair cycle time** and **21% reduction in material consumption**. The latter directly translates to lower consumption of expensive alloying elements and filler materials, yielding significant cost savings and supporting sustainability objectives through reduced material waste and energy expenditure per repair cycle.

Importantly, these findings contribute directly to the most recent developments and literature in the field. Recent works by Hackenhaar et al., Tanvir et al., Wang et al., and Baffa et al. collectively demonstrate rapid advancements in WAAM for tool steel applications, from process parameter optimization and microstructure control to repair strategies for complex die geometries [41–44]. The present study extends these advances by offering a holistic, systematic validation of WAAM, not only in controlled laboratory settings but also through real-world industrial testing - a crucial step beyond purely academic studies that often lack practical verification under operational conditions..

In summary, our results advance the current state-of-the-art in several key areas:

- They confirm the ability of optimized WAAM processes to deliver superior wear resistance compared to wrought H11 reference material and conventional GMAW repair methods.
- They provide, for the first time, direct industrial evidence of the process's substantial economic and operational benefits—including extended tool durability, reduced repair time, and lower material consumption—compared to standard GMAW-based repairs.
- They highlight the suitability of WAAM for complex geometries and high-performance requirements in hot forging, aligning with the circular economy and sustainability objectives that are increasingly critical in modern manufacturing..

Further work is recommended to explore the transferability of these gains to additional process conditions, tool geometries, and longer-term service exposures, thereby broadening the industrial applicability of WAAM.

Funding This research received funding from the European Union's Horizon 2020 research and innovation programme under grant agreement No 862017.

Data availability Data will be made available on reasonable request.

Declarations

Conflict of interest The authors declare that they have no known competing financial interests or personal relationships that could have appeared to influence the work reported in this paper. On behalf of all authors, the corresponding author states that there is no conflict of interest.

References

1. Widomski P, Gronostajski Z. Comprehensive review of methods for increasing the durability of hot forging tools. Procedia Manuf. 2020;47:349–355. https://doi.org/10.1016/j.promfg.2020.04.280.
2. Ahn D-G. Hardfacing technologies for improvement of wear characteristics of hot working tools: a review. Int J Precis Eng Manuf. 2013;14:1271–83. https://doi.org/10.1007/s12541-013-0174-z.
3. Lange K, Cser L, Geiger M, Kals JAG. Tool life and tool quality in bulk metal forming. CIRP Ann. 1992;41:667–75. https://doi.org/10.1016/S0007-8506(07)63253-3.
4. Emamverdian AA, Sun Y, Cao C, Pruncu C, Wang Y. Current failure mechanisms and treatment methods of hot forging tools (dies) - a review. Eng Fail Anal. 2021;129:105678. https://doi.org/10.1016/j.engfailanal.2021.105678.
5. Euroforge IS. 2023-2, https://www.euroforge.org/wp-content/uploads/2023/09/International-Statistics-2023-2.pdf, (n.d.).
6. Singh AK. Factors affecting die wear. Wear. 1973;25:271–9. https://doi.org/10.1016/0043-1648(73)90077-X.
7. Wanheim T, Bay N, Petersen AS. A theoretically determined model for friction in metal working processes. Wear. 1974;28:251–8. https://doi.org/10.1016/0043-1648(74)90165-3.
8. Kchaou M, Elleuch R, Desplanques Y, Boidin X, Degallaix G. Failure mechanisms of H13 die on relation to the forging process – a case study of brass gas valves. Eng Fail Anal. 2010;17:403–15. https://doi.org/10.1016/j.engfailanal.2009.08.015.
9. Kim DH, Lee HC, Kim BM, Kim KH. Estimation of die service life against plastic deformation and wear during hot forging processes. J Mater Process Technol. 2005;166:372–80. https://doi.org/10.1016/j.jmatprotec.2004.07.103.
10. Kang JH, Park IW, Jae JS, Kang SS. A study on die wear model considering thermal softening (II): application of the suggested wear model. J Mater Process Technol. 1999;94:183–8. https://doi.org/10.1016/S0924-0136(99)00104-1.
11. Sharma R, Arrowsmith DJ. The wear of forging dies in the first five forging blows. Wear. 1981;74:1–10. https://doi.org/10.1016/0043-1648(81)90190-3.
12. Summerville E, Venkatesan K, Subramanian C. Wear processes in hot forging press tools. Mater Des. 1995;16:289–94. https://doi.org/10.1016/0261-3069(96)00010-6.
13. Gronostajski Z, Kaszuba M, Hawryluk M, Zwierzchowski M. A review of the degradation mechanisms of the hot forging tools. Arch Civ Mech Eng. 2014;14:528–39. https://doi.org/10.1016/j.acme.2014.07.002.
14. Lv L, Deng Z, Liu T, Wan L, Huang W, Yin H, Zhao T. A composite evaluation model of sustainable manufacturing in machining process for typical machine tools. Processes. 2019;7:110. https://doi.org/10.3390/pr7020110.
15. Ong SK, Fang HC, Nee AYC. A design feature-based approach for product remanufacturability assessment and analysis. Procedia CIRP. 2016;53:15–20. https://doi.org/10.1016/j.procir.2016.07.005.
16. Reike D, Vermeulen WJV, Witjes S. The circular economy: new or refurbished as CE 3.0? — exploring controversies in the conceptualization of the circular economy through a focus on history and resource value retention options. Resour Conserv Recycl. 2018;135:246–64. https://doi.org/10.1016/j.resconrec.2017.08.027.
17. Velte C.J., Scheller K., Steinhilper R. Circular economy through Objectives – Development of a proceeding to understand and shape a circular economy using Value-focused thinking. Procedia CIRP. 2018;69:775–80. https://doi.org/10.1016/j.procir.2017.11.031.
18. Rahito D, Wahab A, Azman. Additive manufacturing for repair and restoration in remanufacturing: an overview from object design and systems perspectives. Processes. 2019;7:802. https://doi.org/10.3390/pr7110802.
19. Paterson DAP, Ijomah WL, Windmill JFC. End-of-life decision tool with emphasis on remanufacturing. J Clean Prod. 2017;148:653–64. https://doi.org/10.1016/j.jclepro.2017.02.011.
20. Pytel S, Turek J, Okoński S, Zarębski K. The properties and microstructure of padding welds built up on the surface of forging dies. Arch Foundry Eng. 2010;10:5–10. http://www.afe.polsl.pl/index.php/pl/magazine/show/64/volume-10-special-issue-3-2010.

21. Balu CU, Daijo PO, Faizal KPS, Rinson TO, Salim J, Sigimon T, Mathew. Welding life enhancement of steel forging dies. Int J Adv Eng Glob Technol. 2016;4:1771–9.
22. Farhani M, Amadeh A, Kashani H, Saeed-Akbari A. The study of wear resistance of a hot forging die, hardfaced by a cobalt-base Superalloy. Mater Forum. 2006;30:212–8.
23. Kashani H, Amadeh A, Ghasemi HM. Room and high temperature wear behaviors of nickel and Cobalt base weld overlay coatings on hot forging dies. Wear. 2007;262:800–6. https://doi.org/10.1016/j.wear.2006.08.028.
24. Bayramoglu M, Polat H, Geren N. Cost and performance evaluation of different surface treated dies for hot forging process. J Mater Process Technol. 2008;205:394–403. https://doi.org/10.1016/j.jmatprotec.2007.11.256.
25. Ahn D-G, Lee H-J, Cho J-R, Guk D-S. Improvement of the wear resistance of hot forging dies using a locally selective deposition technology with transition layers. CIRP Ann. 2016;65:257–60. https://doi.org/10.1016/j.cirp.2016.04.013.
26. Kim D-I, Jang Y-H, Lee H-J, Ahn D-G, Song H, Seok C-S. Design of overlay coated region with hardfacing, transition and damage diminution layers for the reduction of damages of hot forging tools. J Mech Sci Technol. 2017;31:5639–47. https://doi.org/10.1007/s12206-017-1104-2.
27. Gao F, Zhou J, Zhou J, Shen L, Zhang J, Tao Y, Li M. Microstructure and properties of surfacing layers of dies manufactured by bimetal-gradient-layer surfacing technology before and after service. Int J Adv Manuf Technol. 2017;88:1289–97. https://doi.org/10.1007/s00170-016-8679-0.
28. Shen L, Zhou J, Xiong Y-B, Zhang J-S, Meng Y. Analysis of service condition of large hot forging die and refabrication of die by bimetal-layer weld surfacing technology with a cobalt-based Superalloy and a ferrous alloy. J Manuf Process. 2018;31:731–43. https://doi.org/10.1016/j.jmapro.2018.01.005.
29. Junker D, Hentschel O, Schmidt M, Merklein M. Investigation of heat treatment strategies for additively-manufactured tools of X37CrMoV5-1. Metals. 2018;8:854. https://doi.org/10.3390/met8100854.
30. Hentschel O, Siegel L, Scheitler C, Huber F, Junker D, Gorunow A, et al. Processing of AISI H11 tool steel powder modified with carbon black nanoparticles for the additive manufacturing of forging tools with tailored mechanical properties by means of laser metal deposition (LMD). Metals. 2018;8:659. https://doi.org/10.3390/met8090659.
31. Wang S, Lu H, Shu F, Zhang X, Li G. Bonding mechanism between the AlN ceramic matrix and the copper-based metal cladding layer. Mater Sci-Poland. 2025;43:42–50. https://doi.org/10.2478/msp-2025-0004.
32. Junker D, Hentschel O, Schramme R, Schmidt M, Merklein M. Performance of hot forging tools built by laser metal deposition of hot work tool steel X37CrMoV5-1. in: Lasers Manuf Conf, 2017: pp. 1–9.
33. Corbin S. Control of Laser Cladding Process. In: Laser Cladding. CRC Press; 2004. https://doi.org/10.1201/9781420039177.ch5.
34. Müller B, Hund R, Malek R, Gerth N. Laser Beam Melting for Tooling Applications – New Perspectives for Resource-Efficient Metal Forming and Die Casting Processes, in: 2013: pp. 124–137. https://doi.org/10.1007/978-3-642-41329-2_14
35. Muller B, Gebauer M, Hund R, Malek R, Gerth N. Metal additive manufacturing for tooling applications - Laser beam melting technology increases efficiency of dies and molds. in: Met Addit Manuf Conf, 2014: pp. 1–14. http://publica.fraunhofer.de/dokumente/N-322053.html
36. Tang Z, Li W, Yang Z, Wang J. Effect of solution and artificial aging heat treatment on the hardness, friction and wear properties of laser cladding and roll-formed 18Ni300 materials. Mater Sci-Poland. 2024;42:26–40. https://doi.org/10.2478/msp-2024-0017.
37. Samodurova MN, Chumanov IV, Anikeev AN, Shaburova NA, Pashkeev KY, Nurkenov AK, Zakirov RA, Latfulina YS. Restoration of die equipment by laser cladding using robotic complex FL-CLAD–R-4. Metallurgist. 2021;64:1086–95. https://doi.org/10.1007/s11015-021-01090-4.
38. Wang J, Zhang B, Tang H, Wei X, Hao W, Wang J. Development of integrated automatic system of laser cladding for repairing of polycrystalline diamond compact bits. Electronics. 2023. https://doi.org/10.3390/electronics12040900.
39. Yeo NCY, Pepin H, Yang SS. Revolutionizing technology adoption for the remanufacturing industry. Procedia CIRP. 2017;61:17–21. https://doi.org/10.1016/j.procir.2016.11.262.
40. Buchmayr B. Damage, lifetime, and repair of forging dies. BHM Berg- und Hüttenmänn Monatsch. 2017;162(3):88–93.
41. Kaszuba MD, Widomski P, Kiełczawa T, Gronostajski Z. The use of a measuring arm with a laser scanner for analysis and support of regenerative surfacing processes of forging dies. Weld Tech Rev. 2020;92(3):23–32. https://doi.org/10.26628/wtr.v92i3.1103.
42. Lisiecka-Graca P, Lisiecki Ł, Zyguła K, Wojtaszek M. Evaluation of cracking risk of 80MnSi8-6 nanobainitic steel during hot forging in the range of lower temperature limits. Mater Science-Poland. 2024;42:171–85. https://doi.org/10.2478/msp-2024-0011.
43. Kim J-D, Kim JW, Cheon JY, Kim Y-D, Ji C. Effect of shielding gases on the wire arc additive manufacturability of 5 cr–4 mo tool steel for die casting mold making. Korean J Met Mater. 2020;58(12):852–62. https://doi.org/10.3365/KJMM.2020.58.12.852.
44. Hackenhaar W, Mazzaferro JA, Mazzaferro CC, Grossi N, Campatelli G. Effects of different Waam current deposition modes on the mechanical properties of AISI h13 tool steel. Weld World. 2022;66(11):2259–69. https://doi.org/10.1007/s40194-022-01342-0.

45. Tanvir ANM, Ahsan MR, Seo G, Bates B, Lee C, Liaw PK, Noakes M, Nycz A, Ji C, Kim DB. Phase stability and mechanical properties of wire + arc additively manufactured h13 tool steel at elevated temperatures. J Mater Sci Technol. 2021;67:80–94.
46. Wang T, Zhang Y, Wu Z, Shi C. Microstructure and properties of die steel fabricated by WAAM using H13 wire. Vacuum. 2018;149:185–9. https://doi.org/10.1016/j.vacuum.2017.12.034.
47. Baffa F, Venturini G, Campatelli G, Galvanetto E. Effect of stepover and torch tilting angle on a repair process using WAAM. Adv Manuf. 2022;10(4):541–55. https://doi.org/10.1007/s40436-022-00393-2.
48. Drozd K, Walczak M, Szala M, Gancarczyk K. Tribological behavior of AlCrSiN-coated tool steel K340 versus popular tool steel grades. Materials. 2020;13:4895. https://doi.org/10.3390/ma13214895.

Authors and Affiliations

Pawel Widomski[1] · Marcin Kaszuba[1] · Maciej Zwierzchowski[1] · Constantinos Goulas[2] · Martijn Bos[2] · Marcel Hermans[3]

✉ Pawel Widomski
pawel.widomski@pwr.edu.pl

[1] Faculty of Mechanical Engineering Department of Metal Forming, Welding and Metrology , Wrocław University of Science and Technology , Wrocław, Poland

[2] University of Twente , Twente, Netherlands

[3] Delft University of Technology , Delft, Netherlands